2020 IEEE International Conference on Robotics and Automation (ICRA)
31 May - 31 August, 2020. Paris, France

Design and Analysis of a Synergy-Inspired Three-Fingered Hand

Wenrui Chen, Zhilan Xiao, Jingwen Lu, Zilong Zhao, and Yaonan Wang

Abstract—**Hand synergy from neuroscience provides an effective tool for anthropomorphic hands to realize versatile grasping with simple planning and control. This paper aims to extend the synergy-inspired design from anthropomorphic hands to multi-fingered robot hands. The synergy-inspired hands are not necessarily humanoid in morphology but perform primary characteristics and functions similar to the human hand. At first, the biomechanics of hand synergy is investigated. Three biomechanical characteristics of the human hand synergy are explored as a basis for the mechanical simplification of the robot hands. Secondly, according to the synergy characteristics, a three-fingered hand is designed, and its kinematic model is developed for the analysis of some typical grasping and manipulation functions. Finally, a prototype is developed and preliminary grasping experiments validate the effectiveness of the design and analysis.**

I. Introduction

Robotic hands have been developed with the aim of matching the human hand in terms of dexterity and adaptation capabilities to equip either a dexterous manipulator or human being with a prosthetic device. To adapt hands to the many kinds of tasks, multiple degrees of freedom (DOFs) distributed among several fingers are needed. A classic design approach attempts to closely replicate the appearance and dexterity of human hands with sophisticated designs integrating many actuators and sensors [1, 2]. Since it is overly complex to seek perfect structural and functional anthropomorphism, this approach has resulted in a limited number of real-world applications. Some recent innovations in hand design aim at achieving robust, easily programmable, and economically viable robotic hands while reducing the need for functionality. For examples, many popular robot platforms for the end user still are built with single-actuator grippers such as the Willow Garage PR2, or simplified multi-fingered hands optimized for power grasping configurations such as Barrett Hand and the Robotiq Adaptive Gripper. These hands perform certain grasps robustly with simpler mechanics control, but lose part of the dexterity especially the in-hand manipulation ability. There is still a huge gap between dexterity and practicality that needs to be overcome.

One promising approach to reduce this complexity of hands without compromising dexterity is through *synergy*, which is from neuroscience and shows that a continuous subspace of configuration space can be used to approximate everyday human hand tasks [3, 4]. Human hand synergy provides a natural modeling paradigm for robotics. For example, synergies can be used in the planning or control algorithms for fully-actuated hands[5]. In addition, this notion can be embedded in the mechanical design of hands via coupling joints, moving some of the control intelligence to the physical mechanism. Brown and Asada designed a mechanical hand to restructure the first two hand posture synergies via two actuators driving 17 joints of the whole hand [6]. Different types of mechanisms also were proposed to enable hardware synergies for anthropomorphic hands[7-9]. To deal with the force issue in postural synergies, the concept of "soft synergies" was presented and the models and tools were provided to account for force generation and force equilibrium [10]. Based on this theory, the Pisa/IIT hand is developed [11]. In our previous work [12], a mechanical implementation method of the complete statistical information of human hand synergies was presented where the few-order hand synergies are achieved via actuators while the high-order hand synergies are implemented with mechanical compliance. This method is used in the design of an anthropomorphic hand [8]. Intrinsically, these mechanical implementations of human hand synergies are based on compliant and underactuated mechanisms. Meanwhile, the human hand synergy provides a new inspiration for underactuated hand design overcoming the huge gap between dexterity and complexity.

This paper aims to extend the synergy inspired design from anthropomorphic hands to multi-fingered robot hands. This robot hands are not necessarily humanoid in morphology but perform primary functions of the human hand. Specifically, a three-fingered hand is designed according to the human hand synergy. At first, the biomechanical characteristics of hand synergy is explored as a basis for the mechanical simplification of robot hands. According to the characteristics of hand synergy, a three-fingered hand is designed, and its kinematic model is developed for the analysis of the typical grasping and manipulation functions. Finally, a prototype is developed and preliminary experiments validate the effectiveness of the design and analysis.

II. Hand Characteristics and Simplification

The human hand is the best reference for robot hand design. Unlike traditional morphological imitation, we focus on functional humanoids. Based on the analysis of synergistic features and musculoskeletal structure, some characteristics of hand synergy are revealed as a bionic basis for the mechanical simplification of the robot hands.

A. Biomechanical Characteristics of Hand Synergy

The human thumb has three joints: the interphalangeal (IP), the metacarpophalangeal (MCP), and the carpometacarpal (CMC) joint, as shown in Fig. 1. The CMC joint is a compound joint whose two nonorthogonal axes are located in different bones and thus more drastically offset. The CMC

*Research supported by the National Key R&D Program under Grant 2018YFB1308604, the National Natural Science Foundation of China under Grant 61733004, the Hunan Key Laboratory of Intelligent Robot Technology in Electronic Manufacturing under Grant IRT2018005, and the Fundamental Research Funds for the Central Universities under Grant 531107051013.

W. Chen, Z. Xiao, J. Lu, Z. Zhao and Y. Wang are with National Engineering Laboratory for Robot Vision Perception and Control Technology, Hunan University, Changsha 410082, China (e-mail: chenwenrui@hnu.edu.cn; 915383308@qq.com; 545989735@qq.com; 320925825@qq.com; yaonan@hnu.edu.cn).

adduction-abduction (aa) axis passes through the proximal end of the metacarpal bone, while the CMC flexion-extension (fe) axis intersects with the trapezium carpal bone [56]. Each of the fingers has three joints called distal interphalangeal (DIP), proximal interphalangeal (PIP), and MCP joints, respectively. The DIP and PIP joints can generate rotation movement around the axis-fe, while the MCP joint a compound joint whose two orthogonal axes, namely the axis-fe and the axis-aa, respectively, as shown in Fig. 1.

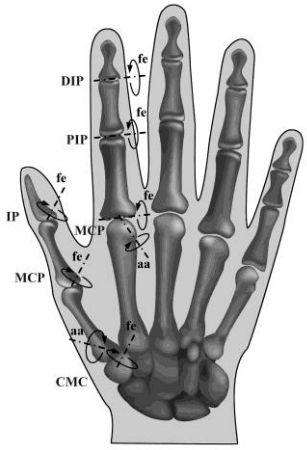

Fig. 1 Joints and rotation movement axes of human hand

Santello et al. [3] investigated grasping posture data from a large set of familiar objects via principal components analysis (PCA) and revealed that more than 80% of hand posture information is contained in the first two principal components. It indicates that the grasping posture can be expressed as a much lower-dimensional subspace of the hand joint space and reflects significant joint coupling and inter-finger coordination. Error analysis [13] shows that the reconstruction of human high-dimensional data with two principal elements has a small overall error, but the error of a single joint is very large. Especially, the errors of the thumb joints reach up to 80%. Such large errors are unacceptable for grasping and in-hand manipulation. The statistics of natural hand movements indicates that there are not only correlation but also independence among hand joints [14]. It represents two forms of synergy, namely *coupling* and *grouping*. Its functional link with human musculoskeletal architecture provides a biomechanical basis for hand synergy [15]. Biomechanical characteristics of hand synergy are mainly manifested in the following.

The adduction-abduction movement is independent with flexion-extension movement. Since the amplitude of the adduction-abduction movement is very small compared to flexion-extension, it is often ignored in the collaborative analysis. Although the adduction-abduction movement is not significant in the synergistic analysis, it is critical to dexterity. Unlike the flexion-extension muscles (such as flexor digitorum profundus (FDP) and flexor pollicis longus (FPL) muscles) distributed in the forearm, the adduction-abduction muscles (such as palmar and dorsal interosseous muscles) are basically distributed in the palm.

Coordination and independence between digits. The thumb is the most independent of the digits. The joints of the thumb have lower coordinated relationships with the joints of the four fingers. The thumb can be able to move independently of the other fingers to perform various tasks. FDP muscle, an important flexor muscle, attaches to the four fingers, while the thumb has a separate long flexor muscle (FPL muscle) in the forearm. In addition, the other multi-tendon muscles only connect the fingers, while the movements of the thumb joints are driven by exclusive muscles. The separate biomechanical structure is reflected in the poor movement-coordinated relationships between the thumb and the fingers. The same muscles connect the fingers and carry out the coordinated movements of the corresponding joints of different fingers.

Coupling and coordination within the fingers. Correlations between the flexion-extension joints within each finger were low for the MCP joint and very high between the PIP and DIP joints. The movements of the MCP joints have a significant difference with the PIP and DIP joints. The flexion motions of the MCP, DIP and PIP joints of each finger are primarily due to the separate actions of the FDP and FDS muscles. The compound tendinous attachments of the extensor expansion connect the PIP and DIP joints and make the two joints rotate as a mechanism with one degree of freedom when the FDP is active [16]. Except for the same muscles for the PIP and DIP joints, such as the FDP and FDS muscles, the particular lumbrical muscles for the MCP joints increase the diversity of movement and result in the relative independence of the MCP joints compared to the PIP and DIP joints of the four fingers. These anatomical structures lead to the PIP and DIP joints of the four fingers more coordinated than the MCP joins.

It is worth noting that the musculoskeletal system is far more complicated than described above. What has been described above is the main aspect related to synergy.

B. Hand Topological Structure

The human hand synergy reflects the simplification of the control strategy. Attempts to formalize human tendency to simplify the space of possible grasps can be traced back to Napier's pioneering grasp taxonomy [17], which divided grasps into power and precision grasps. With similar consideration, Iberall introduced the concept of "virtual fingers", in which each virtual finger represents all of the fingers that are controlled as one unit in a grasping process [18]. In studying the grasps for manufacturing tasks, Cutkosky showed a grasp hierarchy which offers a classification scheme for typical human grasps [19]. Fiex extended the taxonomy for manufacturing to one for the activities of daily living [20]. A total of 33 different grasp types are identified and arranged in the comprehensive taxonomy.

In all 33 types of Fiex's grasping taxonomy, the thumb is used in 32 types, the index finger is used in 33 types, and the middle finger is used in 28 types. The thumb, index finger and middle finger are used at the same time in 27 types. In each of the grasping taxonomy, there are at least two digits used among the thumb, index finger and middle finger. It is not hard to find that in the daily activities, the thumb, index finger and middle finger are used most frequently, and bear the most important grasping task. Statistically, three digits cover the vast majority of grasping types. Hence, we adopt three digits in the designed hand, as shown in Fig. 2. Each digit has a joint for adduction-abduction and three joints for flexion-extension.

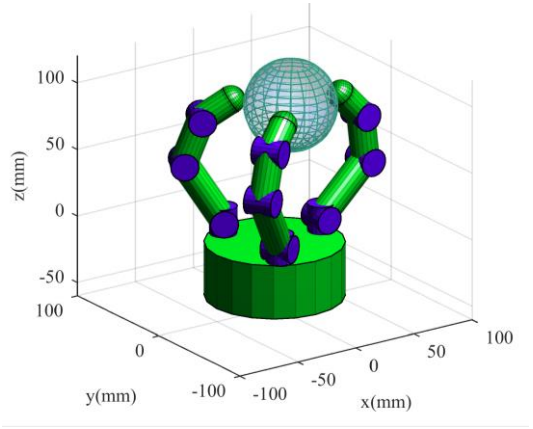

Fig. 2 Joint arrangement of the robot hand.

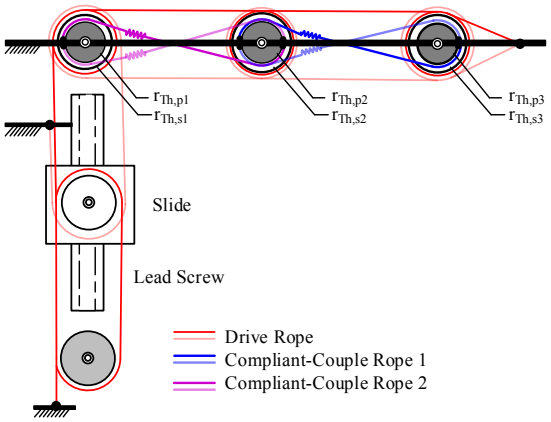

Fig. 3 The transmission for flexion-extension of the thumb.

III. Transmission Design and Kinematic Analysis

The design of robot hand is to reproduce the hand synergy of the human hand. As mentioned in Section II-A, there exist three biomechanical characteristics of hand synergy.

- The adduction-abduction movement is independent with flexion- extension movement;
- The thumb is independent with the other fingers, while the corresponding joints of different fingers movements synchronously;
- The PIP and DIP joints of a finger more coordinated than the MCP joint.

Hence, in the robot hand, there are three independent transmission modules described as following.

A. *Flexion-extension of the Thumb for Inner-Fingered Adaptability.*

The three flexion-extension joints of the thumb, $\mathbf{q}_{Th}=\begin{bmatrix} q_{Th1} & q_{Th2} & q_{Th3}\end{bmatrix}^T$, are driven by an actuator a_{Th} through a tendon-driven differential transmission with two compliant couples shown in Fig. 3. The transmission functions $\mathbf{T}_{Th}(\mathbf{q},\mathbf{a})$ are expressed as

$$\begin{cases} T_{Th,s}=\mathbf{J}_{Th,s}\mathbf{q}_{Th}-2a_{Th} \\ \mathbf{T}_{Th,p}=\mathbf{J}_{Th,p}\mathbf{q}_{Th} \end{cases} \tag{1}$$

where the deformation of the tendon $T_{Th,s}$, the deformations of two groups of coupling springs $\mathbf{T}_{Th,p}=\begin{bmatrix} T_{Th,p1} & T_{Th,p2}\end{bmatrix}^T$, and

$$\mathbf{J}_{Th,s}=\begin{bmatrix} r_{Th,s1} & r_{Th,s2} & r_{Th,s3}\end{bmatrix}$$

$$\mathbf{J}_{Th,p}=\begin{bmatrix} r_{Th,p1} & -r_{Th,p2} & 0 \\ 0 & r_{Th,p2} & -r_{Th,p3}\end{bmatrix}$$

Then, from the virtual work principle, the *equilibrium equation* of this transmission mechanism is given as

$$\begin{bmatrix}\boldsymbol{\tau}_{Th} \\ f_{Tha}\end{bmatrix}=\begin{bmatrix}\mathbf{J}_{Th,s}^T & \mathbf{J}_{Th,p}^T \\ -2 & \mathbf{0}\end{bmatrix}\begin{bmatrix}f_{Ths} \\ \mathbf{f}_{Thp}\end{bmatrix} \tag{2}$$

where $\mathbf{f}_{Th,s}$ is a force generated in the serial transmission, $\mathbf{f}_{Th,p}$ is a force generated in the parallel transmission, $\mathbf{f}_{aTh}$ is the actuator force, and $\boldsymbol{\tau}_{Th}$ is the external force described in joint space. The external force is from the contact with the objects in robotic hands.

The elastic potential energy of the thumb can be expressed as

$$V_{Th}(\mathbf{q},\mathbf{a})=\frac{1}{2}\mathbf{T}_{Th}(\mathbf{q},\mathbf{a})^T\mathbf{K}_{ThT}\mathbf{T}_{Th}(\mathbf{q},\mathbf{a}) \tag{3}$$

where $\mathbf{K}_{ThT}=diag(\mathbf{K}_{Ths},\mathbf{K}_{Thp})=diag(k_{Ths},k_{Thp1},k_{Thp2})$. The second order partial derivative of the elastic potential energy with respect to $(\mathbf{q}_{Th},a_{Th})$ is

$$\begin{bmatrix}\delta\boldsymbol{\tau}_{Th} \\ \delta\mathbf{f}_{Tha}\end{bmatrix}=-\frac{\partial^2 V_{Th}}{\partial(\mathbf{q}_{Th},a_{Th})^2}\begin{bmatrix}\delta\mathbf{q}_{Th} \\ \delta a_{Th}\end{bmatrix} \tag{4}$$

where $\dfrac{\partial^2 V_{Th}}{\partial(\mathbf{q}_{Th},a_{Th})^2}=\begin{bmatrix}\mathbf{K}_{Th,q} & \mathbf{K}_{Th,qa} \\ \mathbf{K}_{Th,qa}^T & K_{Th,a}\end{bmatrix}$ is a system stiffness matrix. Then, (4) could be rewritten as

$$\delta\boldsymbol{\tau}_{Th}=-\mathbf{K}_{Th,q}\delta\mathbf{q}_{Th}-\mathbf{K}_{Th,qa}\delta a_{Th} \tag{5}$$

$$\delta f_{Tha}=-\mathbf{K}_{Th,qa}^T\delta\mathbf{q}_{Th}-\mathbf{K}_{Th,a}\delta a_{Th} \tag{6}$$

where

$$\begin{cases}\mathbf{K}_{Th,q}=\mathbf{J}_{Th,s}^T K_{Th,s}\mathbf{J}_{Th,s}+\mathbf{J}_{Th,p}^T\mathbf{K}_{Th,p}\mathbf{J}_{Th,p} \\ K_{Th,a}=K_{Th,s} \\ \mathbf{K}_{Th,qa}=-\mathbf{J}_{Th,s}^T K_{Th,s}\end{cases}$$

Since the system stiffness matrixes are all nothing to do with joint angles and actuator coordinates, the relationship of forces and coordinates of the transmission mechanism can be expressed compactly as

$$\begin{bmatrix}\boldsymbol{\tau}_{Th} \\ f_{aTh}\end{bmatrix}=-\begin{bmatrix}\mathbf{K}_{Th,q} & \mathbf{K}_{Th,qa} \\ \mathbf{K}_{Th,qa}^T & K_{Th,a}\end{bmatrix}\begin{bmatrix}\mathbf{q}_{Th} \\ a_{Th}\end{bmatrix} \tag{7}$$

Note the initial actuator coordinate and the initial joint angles are zero. The matrix $\mathbf{K}_{Th,q}$ is positive definite, so the thumb is stable. Meanwhile, the positive definite stiffness matrix ensures the flexibility of the thumb in all directions.

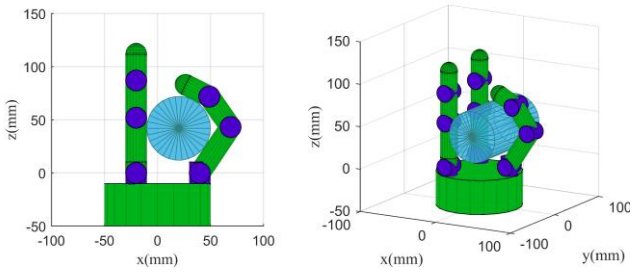

Fig. 4 The thumb adapts to a cylinder.

During free motion before contacting with environment, $\boldsymbol{\tau}_{Th}=\mathbf{0}$. Substituting $\boldsymbol{\tau}_{Th}=\mathbf{0}$ into (7), the free motion can be gotten

$$\Delta\mathbf{q}_{Th}=-\mathbf{K}_{Th,q}^{-1}\mathbf{K}_{Th,qa}\Delta a_{Th}$$

$$\begin{bmatrix}\Delta q_{Th1}\\ \Delta q_{Th2}\\ \Delta q_{Th3}\end{bmatrix}=\frac{2\Delta a_{Th}}{\frac{r_{Th,s1}}{r_{Th,p1}}+\frac{r_{Th,s2}}{r_{Th,p2}}+\frac{r_{Th,s3}}{r_{Th,p3}}}\begin{bmatrix}1/r_{Th,p1}\\ 1/r_{Th,p2}\\ 1/r_{Th,p3}\end{bmatrix} \tag{8}$$

The actuation force during free motion can be gotten

$$f_{Tha}=\left(\mathbf{K}_{Th,qa}^{T}\mathbf{K}_{Th,q}^{-1}\mathbf{K}_{Th,qa}-K_{Th,a}\right)\Delta a_{Th}=0 \tag{9}$$

It means that the actuator does not need to counteract the elastic force in free motion. This mechanism has good transfer characteristics of force and motion[21]. In most underactuated hands such as the hands in [22] and [23], the actuators have to provide some energy to resist the elastic resistance.

The flexion-extension movement of the thumb is driven by the actuator a_{Th}. According to (8) and (9), during free motion before contacting with environment, the thumb moves along the line in (8) without overcoming the elastic resistance in the transmission. After contacting with environment, the thumb can adapt to the environment constraint such as a grasped object in Fig. 4.

B. *Flexion-extension of the two fingers for Inter-Fingered Adaptability.*

The 6 flexion- extension joints of the other two fingers

$$\mathbf{q}_F=\begin{bmatrix}q_{F11} & q_{F12} & q_{F13} & q_{F21} & q_{F22} & q_{F23}\end{bmatrix}^T$$

driven by two actuators $\mathbf{a}_F=\begin{bmatrix}a_{F1} & a_{F2}\end{bmatrix}^T$ through two tendon-driven differential transmissions with four compliant couples shown in Fig. 5. The transmission functions $\mathbf{T}_F(\mathbf{q},\mathbf{a})$ are expressed as

$$\begin{cases}\mathbf{T}_{F,s}=\mathbf{J}_{F,s}\mathbf{q}_F-\mathbf{a}_F\\ \mathbf{T}_{F,p}=\mathbf{J}_{F,p}\mathbf{q}_F\end{cases}$$

where the tendon elongations $\mathbf{T}_{F,s}=\begin{bmatrix}T_{F,s1} & T_{F,s2}\end{bmatrix}^T$, the deformation of parallel springs

$\mathbf{T}_{F,p}=\begin{bmatrix}T_{F,p1} & T_{F,p2} & T_{F,p3} & T_{F,p4}\end{bmatrix}^T$ and

$$\mathbf{J}_{F,s}=\begin{bmatrix}r_{F,s1} & r_{F,s2} & r_{F,s3} & r_{F,s1} & r_{F,s2} & r_{F,s3}\\ r'_{F,s1} & 0 & 0 & r'_{F,s1} & 0 & 0\end{bmatrix}$$

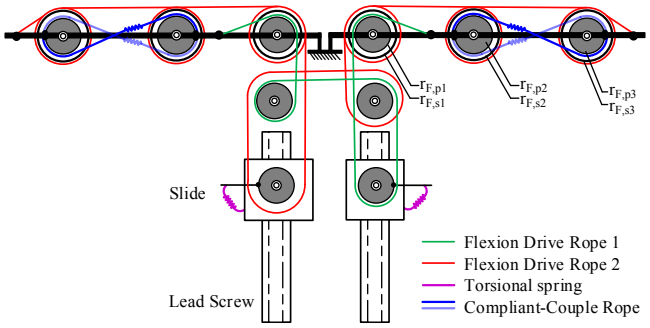

Fig. 5 The transmission for flexion-extension of the two fingers. Note that the extension drive rope 1 and 2, opposite to the corresponding flexion drive rope, are not appeared.

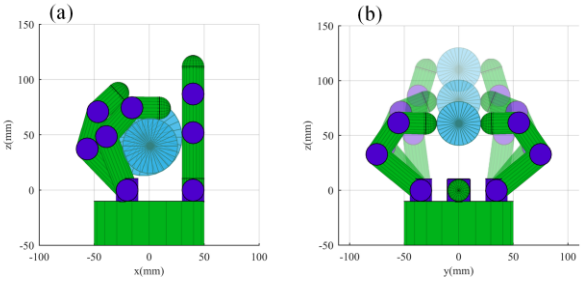

Fig. 6 The two fingers (a) adapt to a multi-diameter shaft, and (b) grasp a sphere of different positions

$$\mathbf{J}_{F,p}=\begin{bmatrix}r_{F,s1} & r_{F,s2} & r_{F,s3} & -r_{F,s1} & -r_{F,s2} & -r_{F,s3}\\ r'_{F,s1} & 0 & 0 & -r'_{F,s1} & 0 & 0\\ 0 & r_{F,p2} & -r_{F,p3} & 0 & 0 & 0\\ 0 & 0 & 0 & 0 & r_{F,p2} & -r_{F,p3}\end{bmatrix}$$

Similar to the thumb, the relationship of coordinates and forces of the transmission mechanism is gotten as following

$$\begin{bmatrix}\boldsymbol{\tau}_F\\ \mathbf{f}_{Fa}\end{bmatrix}=-\begin{bmatrix}\mathbf{K}_{F,q} & \mathbf{K}_{F,qa}\\ \mathbf{K}_{F,qa}^{T} & \mathbf{K}_{F,a}\end{bmatrix}\begin{bmatrix}\Delta\mathbf{q}_F\\ \Delta\mathbf{a}_F\end{bmatrix} \tag{10}$$

where

$$\begin{cases}\mathbf{K}_{F,q}=\mathbf{J}_{F,s}^{T}\mathbf{K}_{F,s}\mathbf{J}_{F,s}+\mathbf{J}_{F,p}^{T}\mathbf{K}_{F,p}\mathbf{J}_{F,p}\\ \mathbf{K}_{F,a}=\mathbf{K}_{F,s}\\ \mathbf{K}_{F,qa}=-\mathbf{J}_{F,s}^{T}\mathbf{K}_{F,s}\end{cases}$$

and

$$\mathbf{K}_{FT}=diag(\mathbf{K}_{Fs},\mathbf{K}_{Fp})=diag(k_{Fs1},k_{Fs2},k_{Fp1},k_{Fp2},k_{Fp3},k_{Fp4})$$

The matrix $\mathbf{K}_{F,q}$ is positive definite, so the fingers are stable. This transmission mechanism of the two fingers has the same transfer characteristics of force and motion as the thumb. The differential transmission during fingers give the hand the inter-fingered adaptability (as shown in Fig. 6(a)), while the two actuators allow the two fingers to grasp objects in different positions, as shown in Fig. 6(b).

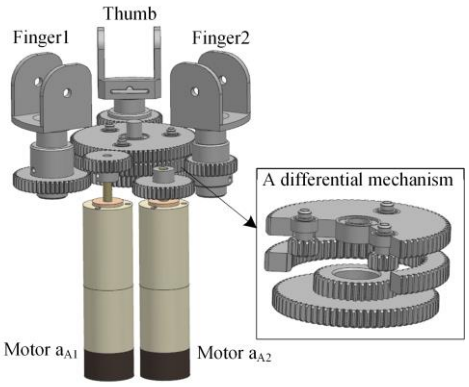

Fig. 7 A gear differential mechanism for 2-DOFs abduction-adduction movements of three digits.

C. 2-DOFs Abduction-Adduction Enhancing Dexterity

The three abduction-adduction joints of the three digits, $\mathbf{q}_A = [q_{A1} \quad q_{A2} \quad q_{A3}]^T$, is driven by $\mathbf{a}_A = [a_{A1} \quad a_{A2}]^T$ through a 2-DOFs gear differential mechanism shown in Fig. 7. We want to achieve two eigen directions (ED) in the abduction-adduction joint space (shown in Fig. 8), namely counter movement of the two fingers (defined as ED1) and the conjugate movement of the three digits (defined as ED2). The eigen directions can be expressed with two vectors, namely $[0 \quad 1 \quad -1]^T$ and $[1 \quad 1 \quad 1]^T$. When the transmission function is designed as

$$\Delta\mathbf{q}_A = \mathbf{J}_A \Delta\mathbf{a}_A \tag{11}$$

where

$$\mathbf{J}_A = \begin{bmatrix} 1 & 0 \\ 0 & 1 \\ 2 & -1 \end{bmatrix}$$

the postures on the two eigen directions can be expressed as

$$\mathbf{q}_{A-E1} = \mathbf{J}_A [0 \quad e_1]^T = e_1 [0 \quad 1 \quad -1]^T$$

$$\mathbf{q}_{A-E2} = \mathbf{J}_A [e_2 \quad e_2 - \pi/3]^T = e_2 [1 \quad 1 \quad 1]^T + [0 \quad -\pi/3 \quad \pi/3]^T$$

where e_1 and e_2 are the coordinates of the corresponding eigen directions, respectively.

The two EDs can be shown in the 2-dimensional actuation space (see Fig. 8), and their linear combination can generate any reachable posture. In particular, some postures with different angles between the digits are generated via the ED1, and the absolute orientations of the digits are determined by the ED2. In Fig. 8, there are three postures on the ED1, namely Posture A where the thumb is parallel to the fingers, Posture B with equal angles between the three digits, Posture C where the thumb is perpendicular to the fingers. The relative angles between the digits remains unchanged, and the three digits synchronously rotate along the ED2, as the three dash-dot lines shown in Fig. 8. Abundant gripping postures and continuous manipulation trajectories can be achieved through the combination of the two EDs.

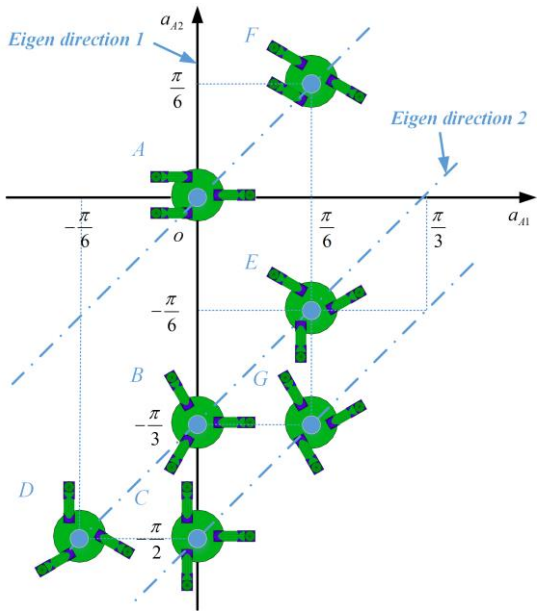

Fig. 8 Eigen directions and some postures of the abduction-adduction joins described in actuator space.

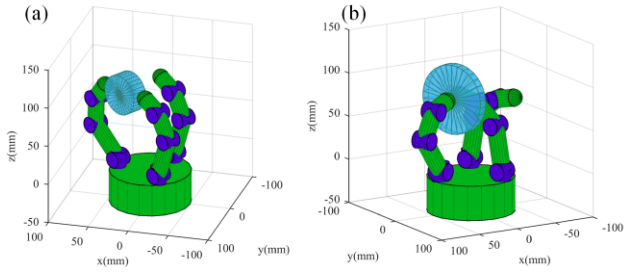

Fig. 9 Two typical grasping postures. (a) Fingertip grasping between the thumb and a finger (corresponds to *Posture F* in Fig. 8), (b) lateral pinch (corresponds to *Posture G* in Fig. 8).

For example, Posture F and Posture G in Fig. 8 are two functional postures generated through the combination of the two EDs. Posture F, an opposite posture of the thumb and a finger, can be used for 2-fingered precision grasping, as shown in Fig. 9(a). The 2-fingered-object plane system in Fig. 9(a) is driven by three actuators a_{Th}, a_{F1} and a_{F2}. Thus, the two fingers can manipulate the grasped object for any motion spanned by two translational movements and one rotational movement in the plane. Posture G, an orthogonal posture of the thumb and a finger, can be used for lateral pinch, as shown in Fig. 9(b).

IV. Experiments

Based on the design and analysis in the above, a synergy-driven three-fingered hand has been developed, as shown in Fig. 10(a). Three DC motors (Maxon DCX19S, gear GPX19 6.6:1, and encoder ENX16) are used to drive the three ball screws (TBI SKF00401) as shown in Fig. 3 and Fig. 5, respectively, to achieve flexion-extension of the three fingers. Two DC motors (Maxon DCX16S, gear GPX16 44:1, and encoder ENX16) are used to drive the gear differential mechanism in Fig. 7 to realize the abduction-adduction movements of the three digits.

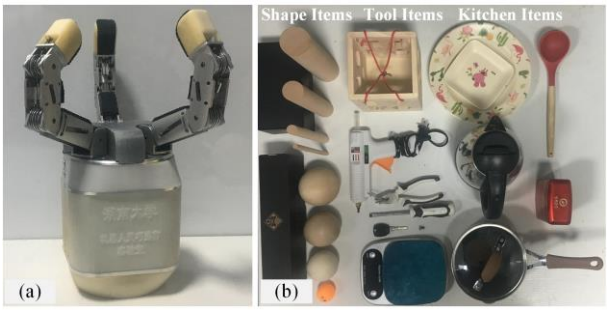

Fig. 10 (a) a synergy-driven three-fingered hand. (b) Objects selected for experiments.

Fig. 11 Grasping demonstration with the prototype. Eight grasping types: H: hook; SG: spherical grip; TP: tripod pinch; EG: extension grip; DVG: diagonal volar grip; LP: lateral pinch; PP: pulp pinch; CG: cylindrical grip. Two non-grasping postures: IP: index pointing/pressing; P: platform.

To evaluate the grasping ability of the synergy-driven three-fingered hand, the Anthropomorphic Hand Assessment Protocol (AHAP) [24] is adopted. The selected objects are similar in shape and function to those used in the Yale-CMU -Berkeley (YCB) dataset for the comparability which are shown in Fig. 10(b). According to the AHAP, eight grasping types and two non-grasping postures (as shown in Fig. 11) are carried out to assess the performance of the developed prototype through grasping score (GS) and maintaining score (MS). The grasping ability score (GAS), the sum of scores of grasping and maintaining. Considering the different number of fingers in different hands, a modified AHAP is presented through changing the Gesture Norm from three fingers at a minimum in contact with objects to two.

The results of both the AHAP and the modified one are shown in Fig. 12, Fig. 13 and TABLE I to more intuitive and fair comparison. It indicates that the modification does not affect the overall test standard. As shown in Fig. 12 and Fig. 13, the prototype is skilled at power grasp such as SG, CG and EG, benefiting from the symmetrical design of finger placement. Meanwhile, the dexterous abduction-adduction of fingers increases the contact surface of finger side (radial and ulnar) with the object, which is useful for hook (H) and lateral pinch (LP) as seen from Fig. 11.

The comparison between the prototype and other artificial hands provided in [24] is shown in TABLE I. According to the primary criterions of the AHAP, all the three scores of the designed three-fingered hand are the highest. Considering the modified AHAP, the mean GS increased, from 64% to 94%, and then the mean GAS increased from 81% to 93%. It means that the functionality of the three-fingered hand is enough to possess the ability to replicate the human-like grasping activities.

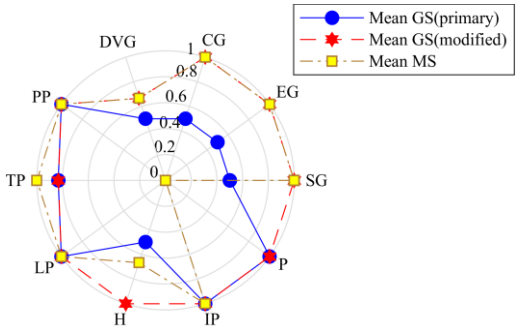

Fig. 12 Mean GS under primary criterions, Mean GS under modified criterions and the Mean MS obtained from the prototype.

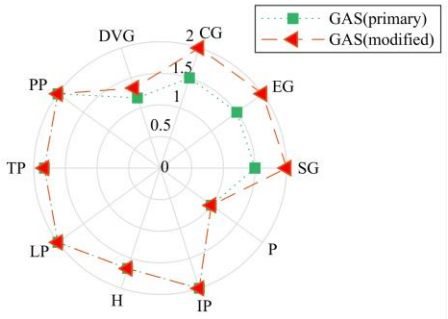

Fig. 13 GAS under primary criterions under modified for each grasp type.

TABLE I COMPARISON OF MEAN GS, MS AND GAS BETWEEN THE PROTOTYPE AND OTHER ARTIFICIAL HANDS

Hand	Grasping	Maintaining	GAS
A1	52%	37%	45%
A2	59%	50%	55%
A3	62%	60%	61%
P1	65%	79%	72%
P2	68%	91%	79%
Prototype	69% 94% (modified)	92%	81% 93%(modified)

V. CONCLUSION AND FUTURE WORKS

This paper examines the synergy of human hands from the perspective of biomechanics. The biomechanical characteristics of hand synergy is summed up as a basis for the design of robot hands to extend the synergy-inspired design from anthropomorphic hands to general robot hands.

Based on the biomechanical characteristics of hand synergy, a three-fingered hand is designed, and its kinematic model is developed for the analysis of the typical grasping and manipulation functions. Preliminary experiment results show that the grasping ability of the designed hand has not inferior to the proposed anthropomorphic hands.

The manipulation ability of the hand will be investigated further. To improve the grasping and manipulation quality of the synergy-inspired hand, it is necessary to optimize mechanism parameters, to add tactile sensors and to develop control algorithms in future work.

REFERENCES

[1] S. C. Jacobsen, J. E. Wood, D. F. Knutti, and K. B. Biggers, "The UTAH/M.I.T. Dextrous Hand: Work in Progress," *The International Journal of Robotics Research,* vol. 3, no. 4, pp. 21-50, 1984.

[2] M. Grebenstein, M. Chalon, W. Friedl, S. Haddadin, T. Wimbock, G. Hirzinger, and R. Siegwart, "The hand of the DLR Hand Arm System: Designed for interaction," *The International Journal of Robotics Research,* vol. 31, no. 13, pp. 1531-1555, 2012.

[3] M. Santello, M. Flanders, and J. F. Soechting, "Postural hand synergies for tool use," *The Journal of Neuroscience,* vol. 18, no. 23, pp. 10105-10115, 1998.

[4] C. R. Mason, J. E. Gomez, and T. J. Ebner, "Hand Synergies During Reach-to-Grasp," *Journal of Neurophysiology,* vol. 86, no. 6, pp. 2896-2910, 2001.

[5] M. T. Ciocarlie and P. K. Allen, "Hand Posture Subspaces for Dexterous Robotic Grasping," *The International Journal of Robotics Research,* vol. 28, no. 7, pp. 851-867, 2009.

[6] C. Y. Brown and H. H. Asada, "Inter-finger coordination and postural synergies in robot hands via mechanical implementation of principal components analysis," in *IEEE/RSJ International Conference on Intelligent Robots and Systems*, San Diego, CA, 2007, pp. 2877-2882.

[7] K. Xu, H. Liu, Y. Du, X. Sheng, and X. Zhu, "Mechanical implementation of postural synergies using a simple continuum mechanism," in *IEEE International Conference on Robotics and Automation*, 2014, pp. 1348-1353: IEEE.

[8] C. Xiong, W. Chen, B. Sun, M. Liu, S. Yue, and W. Chen, "Design and Implementation of Anthropomorphic Hand for Replicating Human Grasping Functions," *IEEE Transactions on Robotics,* vol. 32, no. 3, pp. 652-671, 2016.

[9] W. Chen, C. Xiong, and S. Yue, "Mechanical implementation of kinematic synergy for continual grasping generation of anthropomorphic hand," *IEEE/ASME Transactions on Mechatronics,* vol. 20, no. 3, pp. 1249 - 1263, 2015.

[10] M. Gabiccini, A. Bicchi, D. Prattichizzo, and M. Malvezzi, "On the role of hand synergies in the optimal choice of grasping forces," *Autonomous Robots,* vol. 31, no. 2, pp. 235-252, 2011.

[11] M. G. Catalano, G. Grioli, E. Farnioli, A. Serio, C. Piazza, and A. Bicchi, "Adaptive synergies for the design and control of the Pisa/IIT SoftHand," *International Journal of Robotics Research,* vol. 33, no. 5, pp. 768-782, 2014.

[12] W. Chen, C. Xiong, M. Liu, and L. Mao, "Characteristics analysis and mechanical implementation of human finger movements," in *IEEE International Conference on Robotics and Automation*, Hong Kong, China, 2014, pp. 403-408: IEEE.

[13] M. Liu and C. Xiong, "Synergistic Characteristic of Human Hand during Grasping Tasks in Daily Life," Cham, 2014, pp. 67-76: Springer International Publishing.

[14] J. Ingram, K. Körding, I. Howard, and D. Wolpert, "The statistics of natural hand movements," *Experimental Brain Research,* vol. 188, no. 2, pp. 223-236, 2008.

[15] M. Santello, G. Baud-Bovy, and H. Jörntell, "Neural bases of hand synergies," *Frontiers in Computational Neuroscience,* Review vol. 7, no. 7, pp. 2301-2315, 2013.

[16] H. J. Buchner, M. J. Hines, and H. Hemami, "A dynamic model for finger interphalangeal coordination," *Journal of Biomechanics,* vol. 21, no. 6, pp. 459-468, 1988.

[17] J. R. Napier, "The Prehensile Movements of The Human Hand," *Journal of Bone and Joint Surgery,* vol. 38-B, no. 4, pp. 902-913, 1956.

[18] T. Iberall, "Human Prehension and Dexterous Robot Hands," *The International Journal of Robotics Research,* vol. 16, no. 3, pp. 285-299, 1997.

[19] M. R. Cutkosky, "On grasp choice, grasp models, and the design of hands for manufacturing tasks," *IEEE Transactions on Robotics and Automation,* vol. 5, no. 3, pp. 269-279, 1989.

[20] T. Feix, J. Romero, H. B. Schmiedmayer, A. M. Dollar, and D. Kragic, "The GRASP Taxonomy of Human Grasp Types," *IEEE Transactions on Human-Machine Systems,* vol. 46, no. 1, pp. 66-77, 2016.

[21] W. R. Chen and C. H. Xiong, "On Adaptive Grasp with Underactuated Anthropomorphic Hands," *Journal of Bionic Engineering,* vol. 13, no. 1, pp. 59-72, 2016.

[22] R. Deimel and O. Brock, "A novel type of compliant, underactuated robotic hand for dexterous grasping," in *Robotics: Science and Systems*, Berkeley, CA, 2014, pp. 1687-1692.

[23] L. U. Odhner, L. P. Jentoft, M. R. Claffee, N. Corson, Y. Tenzer, R. R. Ma, M. Buehler, R. Kohout, R. D. Howe, and A. M. Dollar, "A compliant, underactuated hand for robust manipulation," *The International Journal of Robotics Research,* vol. 33, no. 5, pp. 736-752, 2014.

[24] I. Llop-Harillo, A. Pérez-González, J. Starke, and T. Asfour, "The Anthropomorphic Hand Assessment Protocol (AHAP)," *Robotics and Autonomous Systems,* vol. 121, p. 103259, 2019.